Journal of Neurochemistry, 2007, **101**, 506–516 doi:10.1111/j.1471-4159.2007.04473.x

Topological analysis of the complex formed between neurokinin A and the NK2 tachykinin receptor

Sannah Zoffmann,*[,1] Sonia Bertrand,† Quoc-Tuan Do,*[,2] Daniel Bertrand,† Didier Rognan,‡ Marcel Hibert,‡ and Jean-Luc Galzi*

**IFR 85, UMR-CNRS7175, Département Récepteurs et Protéines Membranaires, Ecole Supérieure de Biotechnologie de Strasbourg, Boulevard Sébastien Brant, Illkirch, France*

†Department of Physiologie, Centre Médical Universitaire, rue Michel Servet, Geneva, Switzerland

‡IFR 85, UMR-CNRS7175, Laboratoire de Pharmacochimie de la Communication Cellulaire, Faculté de Pharmacie, route du Rhin, Illkirch, France

Abstract

Neurokinin A stimulates physiological responses in the peripheral and central nervous systems upon interacting primarily with the tachykinin NK2 receptor (NK2R). In this study, the structure of NKA bound to the NK2R is characterised by use of fluorescence resonance energy transfer. Four fluorescent NKA analogues with Texas red introduced at amino acid positions 1, 4, 7 and 10 were prepared. When bound to a NK2R carrying enhanced green fluorescent protein at the N-terminus, all peptides reduce green fluorescent protein fluorescence from 10% to 50% due to energy transfer. The derived donor-acceptor distances are 46, 55, 59 and 69 Å for the fluorophore linked to positions 1–10, respectively. The monotonic increase in distance clearly indicates that the peptide adopts an extended structure when bound to its receptor. The present data are used, in combination with rhodopsin structure, fluorescence studies, photoaffinity labelling and site-directed mutagenesis data to design a computer model of the NKA-NK2R complex. We propose that the N-terminus of NKA is exposed and accessible to the extracellular medium. Subsequent amino acids of the NKA peptide become progressively more buried residues up to approximately one-third of the transmembrane-spanning domain.

Keywords: fluorescence resonance energy transfer, G protein coupled receptor structure, peptide conformation, pharmacology

J. Neurochem. (2007) **101**, 506–516.

Neurokinin A (NKA) also known as substance K is a decapeptide found in the central and peripheral nervous system (Sternini *et al.* 1989; Debeljuk *et al.* 1990). It belongs to the tachykinin peptide family. This widespread group of neuropeptides, found both in invertebrates and vertebrates, also includes substance P (SP) and neurokinin B. All tachykinins share a highly conserved amidated carboxyterminal sequence Phe-X-Gly-Leu-Met-NH_2 (Zhang *et al.* 2000).

NKA is known to act through the G protein-coupled neurokinin receptors. The NK2 receptor (NK2R) is considered as the endogenous receptor for NKA. There is however a high level of promiscuity among tachykinins and their receptors. Indeed, NKA also binds to the NK3 receptor and acts as a high affinity agonist of NK1 receptor through wich it may mediate some its central effects (Beaujouan *et al.* 2000).

The NK2R (Sasai and Nakanishi 1989) is mostly expressed in the peripheral nervous system where it is involved in regulation of gastrointestinal and respiratory systems (Van Schoor *et al.* 1998; Lordal *et al.* 2001). It is expressed at much lower level in the central nervous system (Saffroy *et al.* 2003) where it may mediate NKA anxiolytic effects (Griebel 1999). NK2R may also contribute to central

Received June 19, 2006; revised manuscript received October 4, 2006; Accepted October 16, 2006.

Address correspondence and reprint requests to Jean-Luc Galzi, Ecole Supérieure de Biotechnologie de Strasbourg, Boulevard Sébastien Brant, F-67400 Illkirch, France. E-mail: galzi@esbs.u-strasbg.fr

[1]The present address of Sannah Zoffmann is the Hoffmann-La Roche Ltd., PRBD Grenzacher strasse, Bau 70/4, 4070 Basel, Switzerland.

[2]The present address of Quoc-Tuan Do is the Greenpharma 3, allée du titane, 45100 Orléans, France.

Abbreviations used: DMF, dimthylformamide; FRET, fluorescence resonance energy transfer; GFP, green fluorescent protein; HEK, human embryonic kidney; NBD, nitro benzoxa-diazole; NK2R, neurokinin 2 receptor; NKA, neurokinin A; SP, substance P; TM, transmembrane helix; TmR, tetramethylrhodamine; TmR-ant, TmR-antagonist; TxR, Texas red.

regulation of pain, as shown with the specific-NK2R antagonist SR48968, which reduces neuronal response in the spinal cord to pressure on knee joints in rat (Neugebauer *et al.* 1996). Similar hypoalgesic effect towards moderate to intensive pain was obtained by eliminating the ligand by targeted deletion of the preprotachykinin gene A, which encodes both NKA and SP (Zimmer *et al.* 1998).

Very little information is available about the topology of the NKA-NK2R complex. On one hand, the structure of the NK2R is assumed to adopt a folding similar to that of rhodopsin (Palczewski *et al.* 2000). On the other hand, the structure of NKA appears to be random in water (Gao and Wong 1999) and contains some helical structure in the C-terminal end when it is in contact with sodium dodecyl sulphate or lipid micelles (Whitehead *et al.* 1998; Gao and Wong 1999). Structure-activity relationship studies carried out with NKA analogues support that the conserved C-terminal residues are important for high ligand affinity (Regoli *et al.* 1994; Gembitsky *et al.* 1999).

So far, the only study that orientates part of the ligand towards a specific part of the receptor is based on intermolecular formation of cysteine bridges. It is indeed described that the C-terminal aminoacid of NKA, mutated into a cysteine, forms a cystin bridge with the receptor, when a cysteine is introduced at residue 297 from transmembrane helix (TM) VII (Labrou *et al.* 2001). Other point mutation experiments combined with ^{125}I-NKA binding point toward residues from the outer part of TMIII, -V, -VI and -VII as aminoacids interacting with NKA (Bhogal *et al.* 1994; Renzetti *et al.* 1999; Giolitti *et al.* 2000).

The present study aims at probing the topology of NKA bound to the rat NK2R by measuring intermolecular distances by means of detecting fluorescence resonance energy transfer (FRET) between receptor and ligand. A similar approach aiming at elucidating the structure of a ligand receptor complex has previously been applied to the binding of an antagonist peptide binding the NK2R (Turcatti *et al.* 1996, 1997). In that study, fluorescent receptors incorporating unnatural amino acids were expressed in *Xenopus* oocytes. From FRET efficacy determination, distances from the amino acids to tetramethylrhodamine (TmR) linked to the N-terminus of the antagonist hepta-peptide were estimated (Turcatti *et al.* 1996). This work successfully exploited FRET to demonstrate that peptide antagonists interact with external parts of the hepta-helical domain of the NK2R.

With the introduction of the green fluorescent protein (GFP), it is now possible to produce fluorescent G protein-coupled receptors (Vollmer *et al.* 1999; Kallal and Benovic 2000) in simple expression systems. This allows the detection of receptor interactions with fluorescent ligands, including agonists, by FRET (Vollmer *et al.* 1999; Lecat *et al.* 2002) and thus distance measurements in a system where the receptor is still functional and imbedded in the membrane of intact living cells.

Materials and methods

Preparation of GFP-NK2R

The cDNA for expression of the fluorescent NK2R was prepared and transfected into human embryonic kidney 293 (HEK293) cells as described in Vollmer *et al.* (1999). A cell-line expressing enhanced GFP-NK2R at approximately 1×10^6 sites/cell was established by selection with 600 μg/mL hygromycin and kept in culture in growth medium (minimal essential medium with Earls salts, without L-glutamate) supplied with 10% fetal calf serum, 2 mmol/L glutamate, 50 U/mL penicillin and 50 μg/mL streptomycin) at 37°C, 5% CO_2. Cells were detached with trypsin-EDTA (0.5 g/L trypsin, 500 μmol/L EDTA, 137 mmol/L NaCl, 5 mmol/L KCl, 5 mmol/L D-glucose and 4 mmol/L $NaHCO_3$, pH 7) and diluted twice a week. The stable cell-lines were used for about 12 weeks.

Starting at the N-terminal does the expressed peptide contain: The signal peptide from chicken α7 subunit of the acetylcholine receptor, the GFP amino acids 3–238, a Leu-Tyr-Lys spacer and the rat NK2R (aa 16–390) (Sasai and Nakanishi 1989).

Preparation of fluorescent NK2R ligands

Four fluorescent NKA analogues with Texas red (TxR) linked to amino acid 1, 4, 7 or 10 in the peptide were prepared from the wild-type NKA and three monocysteine substituted peptides: NKA (His-Lys-Thr-Asp-Ser-Phe-Val-Gly-Leu-Met-NH2), NKA[D4C], NKA[V7C] and NKA[M10C]. A peptide NK2R antagonist: PhCO-Lys-Ala-D-Trp-Phe-D-Pro-Pro-Gly-Nle-NH2, was labelled with TmR on the α-aminogroup of lysine by reaction with the isothiocyanate derivative of TmR as described previously (Bradshaw *et al.* 1994). The NKA-wild type was labelled with fluorophore as previously described (Vollmer *et al.* 1999). For the cysteine containing analogues, peptide was dissolved in dimthylformamide (DMF) to a final concentration of 10 mmol/L and supplied with 10 equivalents of triethylamine in DMF. The reagent TxR C5 bromoacetamide in a freshly prepared 30 mmol/L DMF solution was added in two to three steps to finally 0.6–0.9 equivalents. For all five peptides, the progression of the reaction was monitored by reversed-phase HPLC, equipped with C8 column (Zorbax Z5C8 25F; Interchim, Montluçon, France) and detection at two wavelengths 219 and 590 nm (TxR) or 540 nm (TmR). Separation was obtained with a 60 min gradient from 100% solvent A (90% H_2O with 10% acetonitrile) to 100% solvent B (10% H_2O with 90% acetonitrile), both supplied with 0.1% heptafluorobutyric acid for the analytical runs. For isolation of the fluorophore labelled peptide, the reaction was purified in three to five injections. Fractions containing the fluorescent peptide were pooled. The isolated material was reinjected on HPLC with solvent A and B supplemented with trifluoroacetic acid replacing heptafluorobutyric acid, aliquoted and stored at −80°C until use. The purity was verified by analysis of a sample on HPLC and the molecular weight determined by mass-spectroscopic analysis (Matrix Assisted Laser Desorption Ionization Time Of Flight (MALDI TOF)). Experimental molecular weights are as follows: TxR1-NKA: 1865.6 g/mol (expected 1865.3 g/mol); TxR4-NKA: 1852.7 g/mol (expected 1852.5 g/mol); TxR7-NKA: 1868.8 g/mol (expected 1868.1 g/mol); TxR10-NKA: 1837.0 g/mol (expected 1836.1 g/mol) and for the TmR-labelled antagonist (TmR-ant): monoisotopic mass: 1404.60 Da, calculated: 1404.64 Da.

Table 1 K_i and K_d values. Binding affinities for NKA, TxR-NKA analogues and TmR-ant to the GFP-NK2R. K_i values refer to radioligand competition binding (Fig. 2). K_d values refer to direct determination of affinities by fluorescence intensities (Fig. 4)

	Competition [^{3}H]-SR48968			FRET amplitude			Competition [^{125}I]-NKA		
Ligand	K_i (nmol/L)	SEM	*N*	K_d (nmol/L)	SEM	*N*	K_i (nmol/L)	SEM	*N*
NKA	46.5	15.7	9	–	–	–	4.7	3	2
TxR1-NKA	105.4	10	4	21.5	3.3	4	ND*	ND*	
TxR4-NKA	134.6	19.2	4	69.5	46.3	4	16.8	1.5	2
TxR7-NKA	136.8	30.1	3	143.5	41.3	4	44.5	4.4	2
TxR10-NKA	328	120	3	184.4	56.4	4	219.7	85.9	2
TmR-Ant	–	–	–	9.6	3.3	3	–	–	–

*Affinity of bodipy derivative of NKA for NK2R was determined in Vollmer *et al.* (1999) and shown to be equal to that of NKA in competition against [^{125}I] NKA.

FRET, fluorescence resonance energy transfer; GFP, green fluorescent protein; TxR, Texas red; TmR-ant, TmR-antagonist; NKA, neurokinin A.

Concentration of labelled peptides were calculated from the absorbance in methanol at 583 nm using molar extinction coefficient, ε = 113 000/cm/mol/L for TxR labelled-peptides and at 544 nm using ε = 92 000/cm/mol/L for TmR-ant.

Radioligand competition binding

For competition binding with [3H]-SR48963 as tracer, cells were detached at day 1 with trypsin-EDTA, suspended in growth medium and seeded into 96-well plates, with a density of 15–20 000 GFP-NK2R expressing cells/well. On day 2, the competition binding was performed: The cells were washed once in 100μL ice-cold HEPES buffer (137.5 mmol/L NaCl, 1.25 mmol/L $MgCl_2$, 1.25 $CaCl_2$, 6 mmol/L KCl, 5.6 mmol/L glucose, 10 mmol/L HEPES, 1.25 mmol/L NaH_2PO_4 and 1% bovine serum albumin w/v, pH 7.4) and left in 50 μL HEPES buffer supplied with 0.5% protease inhibitors (bestatin, bacitracin, leupeptin, chymostatin and phosphoramidon). To each well, 10 μL of a 10 time concentrated solution of the NKA analogue or the NK2R antagonist SR48968 (gift from Xavier Emonds-Alt, Sanofi-Synthélabo) in 1 m acetic acid was added followed by addition of 40 μL [^{3}H]-SR48968 (27.0 Ci/mmol; Amersham, Buckinghamshire, England) in incubation buffer to a final concentration of 200 pmol/L. The mixture was incubated at 4°C for 3 h and then stopped by two rapid washing steps with 100 μL ice-cold HEPES buffer. The cells were lysed with lysis buffer (3 mol/L acetic acid, 4 mol/L urea and 1% sodium dodecyl sulphate), transferred to vials, supplemented with 2.5 mL scintillation liquid and counted. For competition binding with [125I]-NKA, cells were detached with trypsin-EDTA, washed once with HEPES buffer at 21°C and resuspended in ice-cold HEPES buffer with protease inhibitors. Fifty microlitre containing 25 000 cells were added into a 96-well plate kept on ice (Corning 3600 polystyrene plate; Corning, New York, NY, USA). To each well, 25 μL of a four times concentrated dilution of ligands in HEPES buffer was added, followed by addition of 25 μL [125I]-NKA (2000 Ci/mmol; Amersham) at a final concentration of 0.75 nmol/L. The cells were incubated at 4°C for 3 h and then harvested onto a filter plate (filter plate: Unifilter 96 GF/C, harvester: Unifilter-96 Harvester; both from Perkin Ellmer, Boston, MA, USA) followed by three rapid washing steps with ice-cold buffer. After drying, 50 μL scintilation liquid was added to each filter and the radioactivity was measured.

All measurements were carried out in duplicates and experiments were repeated as indicated in Table 1. Curves were fitted to the experimental values and IC_{50} values determined by use of the software GraphPad Prism version 2.01 (GraphPad Software, San Diego, CA, USA). Calculation of K_d and K_i values was made by use of the Cheng–Prussof equation (Cheng and Prussoff 1973).

Fluorescence measurements

GFP, TxR and TmR fluorescence was measured with a Fluorolog 2 (SPEX; Jobin Yvon, Les Ulis, France) spectrofluorometer equipped with a 450 W Xenon lamp as light source, filtered through a double grating monochromator to a bandwidth of 21.6 nm. Emission wavelength was set with a single grating monochromator and was detected with a photon counting photomultiplier, with a bandwidth at 10.8 nm. Cells were detached with 5 mmol/L EDTA in phosphate-buffered saline and resuspended to a final concentration at 2–4 × 10^6 cells/mL in HEPES-buffer supplied with protease inhibitors (bestatin, bacitracin, leupeptin, chymostatin and phosphoramidon) at 21°C. In general, aliquots of cell suspension were kept at 21°C until use and then transferred to the spectrofluorometer into a 1 mL quartz cuvette thermostated to 21°C and equipped with magnetic stirring.

Time-based recordings of the GFP fluorescence were monitored with excitation wavelength set to 470 nm and emission intensity measured at 510 nm and recorded at 200 ms intervals.

When fluorescence intensity was stabilized, TxR-NKA analogue or TmR-ant was added and the fluorescence intensity was followed until equilibrium was reached (10 min–1.5 h depending on ligand). To reverse the fluorescent ligand binding, an excess of SR48968 (10 μmol/L) was added and the reversal in fluorescence intensity of GFP followed until a plateau was reached.

The protocol was slightly modified for determination binding affinity through saturation binding using FRET. Rather than measuring the association of TxR-NKA or TmR-ant, the fluorescent ligand was added at the chosen final concentration (between 30 nmol/L and 10 μmol/L for TxR-NKA analogues, 3 nm–1 μmol/L for TmR-ant) to the cell sample and incubated at 21°C for a period known to allow equilibrium to be reached. The cell sample was then transferred to the cuvette and the dissociation induced by SR48968 addition was monitored.

The background fluorescence at 510 nm was determined from a sample of non-transfected HEK293 cells diluted to a similar concentration as the suspension of GFP-NK2R expressing cells.

Distance calculation based on FRET efficacy

E, the efficiency of energy transfer, and R_0, the distance at which energy transfer from the donor (GFP) to the acceptor (TxR or TmR) is half-maximal, were estimated as described previously (Lakey *et al.* 1991). R_0 is given by the equation:

$$R_0 = (\mathrm{J}\ \mathrm{K}^2\ \mathrm{Q}_0\ \mathrm{n}^{-4})^{1/6} \times 9.7 \times 10^3\ \text{Å},$$

where K^2 is taken as 2/3 for freely rotating fluorophores and n as 1.4 in aqueous medium. From absorption spectra in methanol and HEPES, the maximal extinction coefficient in HEPES buffer for TxR was found to be 95 600/cm/mol/L at 594 nm and for TmR 55 500/cm/mol/L at 553 nm. The quantum yield $Q_0 = 0.66$ of GFP is taken from the literature (Heim and Tsien 1996). From the calculated overlap integral for the combined emission of GFP and absorbance of TxR ($J = 3.14 \times 10^{-13}$ cm^3/mol/L), the R_0 value was estimated to be 49 Å. For GFP and TmR ($J = 2.10 \times 10^{-13}$ cm^3/mol/L) and the R_0 was estimated to be 53 Å.

Donor–acceptor separation is given by $R = ((\mathrm{E}^{-1}) - 1)^{1/6}\ \mathrm{R}_0$, where E, the maximal efficiency of energy transfer, given by $E = 1\text{-}(\mathrm{F_{DA}}/\mathrm{F_D})$, was determined by measuring specific-donor fluorescence emission in the presence (F_{DA}) and absence (F_D) of ligand at saturating concentrations (300 nmol/L TxR1-NKA, TmR-ant or 1 μmol/L TxR4-NKA, TxR7-NKA and TxR10-NKA). Specific-GFP fluorescence in the absence (F_D) and presence (F_{DA}) of ligand was determined by subtracting auto-fluorescence of non-transfected cells from total fluorescence of GFP-NK2R expressing cells. In a stable cell line selected with 0.5 mg/mL hygromycin for receptor expression is 70–80% of the fluorescence at 510 nm due to GFP-fluorescence.

Creation of model

The rat NK2R sequence was aligned to bovine rhodopsin according to the conserved residues in each transmembrane helices and in external and internal loops (Van Rhee *et al.* 1995). Extensions of the helices were based on their length in rhodopsin. We also did multiple alignments on NK1 and NK2R from rat and human, in order to get structural insights.

The rat NK2R was built by using bovine rhodopsin X-ray structure 1F88 (Palczewski *et al.* 2000) in Sybyl 6.7 package (Tripos, St Louis, MO, USA) with the biopolymer module. The NK2R model was minimised with a maximum number of iterations of 10 000. All the minimisation procedure was undertaken without charge and in Amber 4.1 force field (Fraternali *et al.* 1998) with a maximum of 25 simplex steps coupled to a Powell (Fraternali *et al.* 1998) method, with an energy termination gradient of $0.05 \times \mathrm{kcal} \times \mathrm{mol}^{-1} \times \text{Å}^{-1}$.

Putative interaction sites between NKA and NK2R were identified on an external truncated loop NK2R, by Multi-channel function of the Molcad module and taking into account mutagenesis data from NK1 and NK2R, as well as from ligand analogues (Regoli *et al.* 1990; Bhogal *et al.* 1994; Li *et al.* 1995; Turcatti *et al.* 1997; Holst *et al.* 1998; Gembitsky *et al.* 1999; Labrou *et al.* 1999; Renzetti *et al.* 1999; Giolitti *et al.* 2000; Palczewski *et al.* 2000).

NKA was incrementally (residue by residue) docked into NK2R with the Dock module, starting with the consensus terminal part of the agonist FVGLM according to mutagenesis data and complementary of Molcad lipophilic (Heiden *et al.* 1993) surfaces of the peptide and the receptor, with the N- and C-termini residues capped respectively with amide and carboxamide terminal groups. Studies of NKA in micelle environment by NMR (Whitehead *et al.* 1998) has shown some helical structure in the terminal part of the peptide. However, we could not provide a placement in agreement with the mutagenesis data and the lipophilic complementary surfaces when using helical structure.

A local minimisation was undertaken as described above with the entire NK2R and NKA complex. Following we optimised the placement by using a local molecular dynamic *in vacuo* around NKA at 300 K, NTV constant during 50 ps, with an acquisition time of 50 fs, and Shake algorithm applied on bonds involving hydrogens (Fraternali *et al.* 1998). A bath coupling factor of 100 and 2 fs integration step were used. The whole NKA was grown according to interaction sites identified by mutagenesis data.

TxR-labelled NKA analogues were built starting with the NKA docked in NK2R NK2R. The labelled residue was mutated to cysteine, and TxR joined by adding a bond between *S* and *C* atoms. TxR was positioned considering channels found with Molcad Multi-channel, directing the fluorophore part towards the extra cellular surface, as it is charged. A local minimisation was then undertaken as described above in the Tripos force field (Fraternali *et al.* 1998).

Finally GFP was added, using a GFP-linked muscarinic M1 receptor model (Ilien *et al.* 2003) as a starting placement for the GFP relative to NK2R. Only the centroid of the GFP was considered here. In order to find a set of GFP positions compatible with the four FRET distances, a stochastic search was undertaken to find the best position of the centroid (macro written in SPL). GFP was then positioned according to the best centroid placement found and the linker between GFP and NK2R was built 'manually' by modifying phi and psi torsions of the linker residues. A final minimisation was applied to the whole systems i.e. GFP-NK2R and the different ligands.

Solutions for cell culture were from Invitrogen, Cergy-Pontoise, France; Protease inhibitors from Roche Diagnostics, Meylan, France and ICN Biochemicals, Aurora, Ohio; Fluorescent reagents were from Molecular Probes, Leiden, Netherlands; Solutions for HPLC were from Merck, Darmstadt, Germany; Peptides were from Neosystem, Strasbourg, France.

Results

The efficacy of FRET between two fluorescent groups is dependent on their relative distance. The aim of this study is to make use of this phenomenon to investigate the topology of NKA bound to its cognate NK2R. For this purpose, the NK2R is rendered fluorescent by fusion of its gene to the cDNA encoding GFP, in order to obtain an amino-terminally labelled receptor. This construct was described in a previous work to be fully functional and to exhibit pharmacological properties similar to those of wild-type NK2R (Vollmer *et al.* 1999). The second fluorophore was introduced to the ligand by preparation of four analogues of NKA labelled with the

fluorophore TxR, prepared by chemically linking the fluorophore to the N-terminal aminogroup of NKA or by derivatizing NKA with cysteine substitutions at position 4, 7 or 10. From the literature, it is known that bulky groups can be introduced at the N-terminal end as well as at position 7 without dramatic changes of the pharmacological properties of the ligand (Turcatti *et al.* 1995, 1996; Vollmer *et al.* 1999; Bremer *et al.* 2000). Analogues modified at positions 4 and 10 were included to evenly distribute the fluorophores on the NKA sequence.

In addition, a TmR labelled peptide antagonist (TmR-ant) structurally unrelated to NKA was prepared for the study. The position of TmR in the complex formed between TmR-ant and the NK2R has previously been characterized using FRET-based distance measurements (Turcatti *et al.* 1996).

Distances which can be measured with the GFP-TxR and GFP-TmR FRET approach

The range of distances that can be determined by using GFP and TxR as a donor acceptor pair is illustrated on Fig. 1. From the overlap between the emission spectrum of GFP and absorption spectrum of TxR in assay buffer (Fig. 1a), the distance at which half maximal efficiency of fluorescence energy transfer is expected to occur, corresponds to 47 Å (R_0 value) for freely orienting fluorescent groups. The efficacious range of distances that can be determined with this donor–acceptor pair consequently ranges from approximately 30–75 Å (Fig. 1b). Such distances fall in the range of receptor dimensions. Energy transfer between GFP and TxR is thus expected to be sensitive to distance variations if the fluorophores are moved along NKA sequence.

From the spectral overlap between tetramethyl rhodamin and GFP (not shown) the calculated R_0 value was found to 53 Å, allowing for the use of TmR-ant in combination with our fluorescent GFP-NK2R.

To investigate the effect of TxR addition to the ligand on receptor interaction, two approaches were used. They estimate the binding affinities using the classical radioligand competition-binding assay (indirect affinity determination; KI values) or by using FRET amplitudes to directly derive dissociation constants (KD values).

Radioligand competition binding

Figure 2 illustrates the capacity of NKA, the four TxR-NKA analogues and TmR-ant to compete with [^{3}H]-SR48968 for binding to the GFP-NK2R. Binding experiments were carried out on intact HEK293 cells expressing the receptor at about 10^6 sites/cell (Fig. 2).

All four TxR-NKA ligands compete with SR 48968, with variation in binding affinity lower than one order of magnitude, as compared with NKA. The average K_i values presented in Table 1 show that the largest affinity shift is found for TxR10-NKA, which shows an apparent sevenfold drop in affinity for the NK2R. For TxR1-NKA, TxR4-NKA and TxR7-NKA smaller decreases are observed, as manifested by two to threefold reduction of affinities (Table 1). When competition experiments are carried out using [^{125}I]NKA instead, the amplitude of affinity changes is threefold for NKA derivative carrying TxR at position 4, 10-fold for position 7 and 50-fold for position 10 (Table 1). Although the amplitude of affinity changes is larger than that detected with [^{3}H]SR 48968, the rank order of compounds

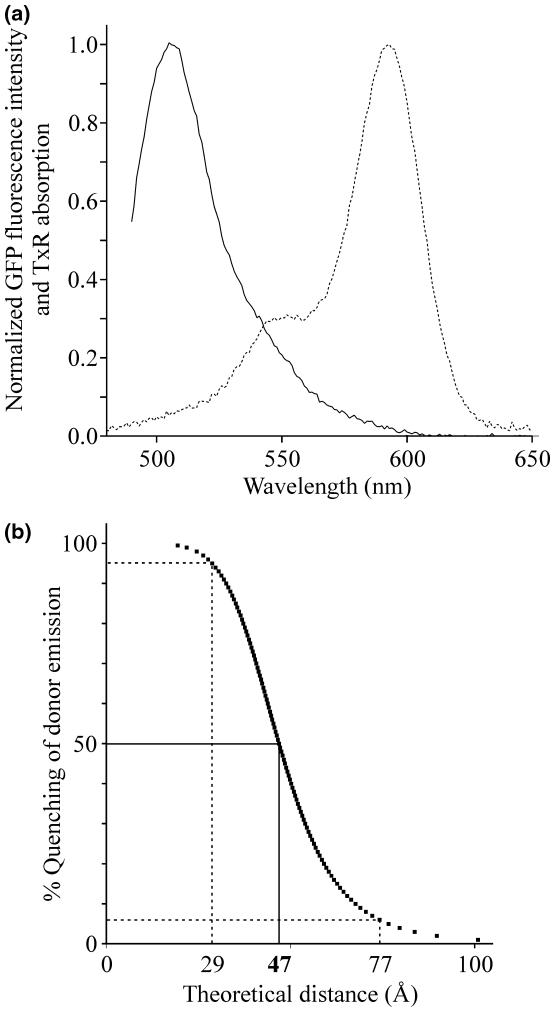

Fig. 1 The distance-range on which fluorescence resonance energy transfer (FRET) between green fluorescent protein (GFP) and Texas red (TxR) may be detected. Panel a: Spectral overlap between donor emission (GFP) and acceptor absorption (TxR). Black line: Normalized emission spectrum for human embryonic kidney 293-GFP-NK2 receptor cells corrected for cell autofluorescence. Broken line: Normalized absorption spectrum for TxR1-neurokinin A in HEPES buffer. Panel b: Theoretical FRET efficacy as a function of donor to acceptor separation in angstrom with determined R_0 = 47 Å. In the figure, the predicted relationship is presented between FRET efficiency (*E*, Y-axis) and distance (*R*, X-axis) between fluorophores, with $R = (1-E^{-1})^{1/6} \times 47$ Å. Distances leading to FRET efficacies of 5%, 50% and 95% are shown.

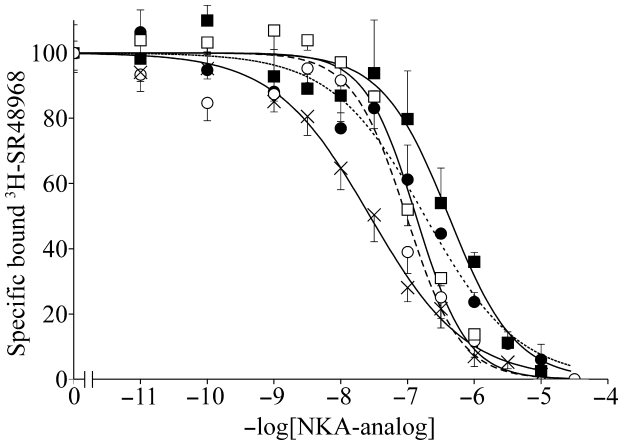

Fig. 2 Radioligand competition binding curves for neurokinin A (NKA) wild-type and the four fluorescent NKA-analogues to green fluorescent protein-NK2 receptor. 3H-SR48968 (0.2 nmol/L) binding to human embryonic kidney 293 cells, stably expressing the receptor was displaced by NKA (open traingles), Texas red (TxR1) -NKA (open circles and broken line), TxR4-NKA (open squares), TxR7-NKA (filled circles and broken line) and TxR10-NKA (filled triangles), at 4°C for 3 h.

binding remains comparable, i.e. moving the fluorophore to more C-terminal positions progressively reduces binding affinity to the NK2R.

Ligand affinity determined from FRET efficacy

The general procedure to measure ligand-receptor interactions is illustrated in Fig. 3. After recording fluorescence of a suspension of cells expressing the GFP-NK2R, the fluorescent NKA derivative was added (Fig. 3a). The interaction of the ligand with the receptor results in a decrease of GFP fluorescence at 510 nm and in an increase of emission at TxR emission wavelength (610 nm). Further addition of an excess (10 μmol/L) of either NKA or SR 48968 reverses the interaction between the fluorescent ligand and the receptor, leading to restoration of initial GFP fluorescence (510 nm) and reduction of TxR fluorescence (610 nm). High concentrations of ligand have been used to ascertain saturation of the receptor sites. Given the high concentrations used, contamination of GFP fluorescence emission by TxR emission was detected beyond 1 μmol/L ligand. Therefore, quantification of receptor sites occupancy was measured, as illustrated in Fig. 3b, by determining the extent of GFP fluorescence recovery after displacement of the fluorescent ligand by a large excess of SR48968. The experimental protocol thus consisted in incubating cells with fluorescent ligand at 21°C for a period necessary to reach equilibrium, (10–25 min, depending on analogue), and then to monitor fluorescent ligand dissociation as shown in Fig. 3b. From the amplitudes of fluorescence variation, the degree of receptor occupancies were determined and plotted as a function of ligand concentration (Fig. 4).

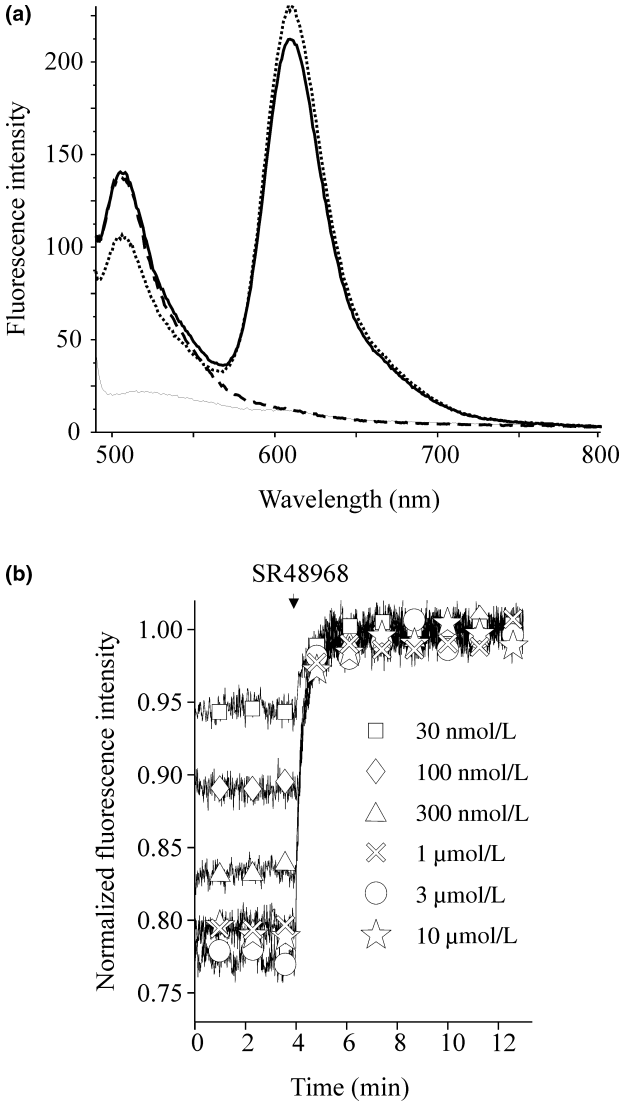

Fig. 3 Fluorescence resonance energy transfer between green fluorescent protein-NK2R (GFP-NK2R) and Texas red-neurokinin A (TxR-NKA) analogues. Panel a: Emission spectra (excitation at 470 nm). Solid broken line: human embryonic kidney 293 cells transfected with GFP-NK2R, 2×10^6 cells/mL corresponding to about 3 nmol/L GFP. Dotted line: GFP-NK2R incubated with 1 μmol/L TxR4-NKA for 20 min. Solid line: Same sample after addition of 10 μmol/L SR48968 and further incubation for 15 min. Thin black line: Fluorescence of a sample of non-transfected cells at identical concentration. Panel b: Example of time-based recording used to determine receptor sites occupancy by TxR7-NKA. Cell samples were incubated with the following concentrations of TxR7-NKA for 15 min: squares: 30 nmol/L; diamonds: 100 nmol/L; triangles: 300 nmol/L; cross: 1 μmol/L; circles: 3 μmol/L and stars: 10 μmol/L. Five minutes after transferring incubated sample to a cuvette, ligand dissociation was initiated by addition of 10 μmol/L SR48968 and fluorescence emission monitored at 510 nm (excitation wavelength 470 nm). Spectra are normalized according to their final value. For the highest concentrations of ligand, (3 and 10 μmol/L) spectra were corrected for shift in intensity due to the small but measurable fluorescence from TxR at 510 nm prior to normalisation.

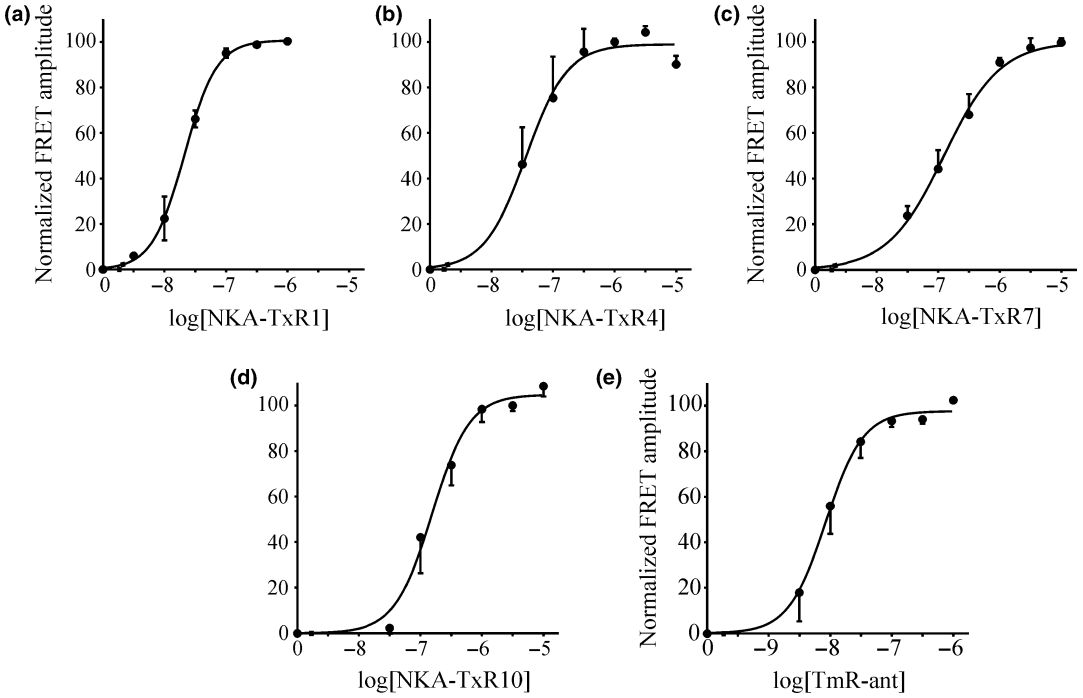

Fig. 4 Direct determination of fluorescent ligands affinity by fluorescence resonance energy transfer (FRET) between green fluorescent protein (GFP) -NK2 receptor and Texas red-neurokinin A (TxR-NKA) analogues. Samples were incubated at 21°C in HEPES buffer with TxR-NKA or TmR-ant until equilibrium was reached. Incubated sample was then transferred to a cuvette and the binding reversed with 10 μmol/L of SR48968. FRET amplitude was monitored as change in GFP fluorescence intensity at 510 nm upon fluorescent ligand dissociation. Panel a: TxR1-NKA, panel b: TxR4-NKA, panel c: TxR7-NKA, panel d: TxR10-NKA and panel e: TmR-ant. The solid line through averaged normalized data from four independent experiments is the best fit with empirical Hill equation.

TxR1-NKA, TxR4-NKA, TxR7-NKA and TxR10-NKA all bind to a saturable population of SR48968 sensitive binding sites. Their apparent dissociation constants for the GFP-NK2R are presented in Table 1. At 1 μmol/L, they occupy a comparable fraction (95 ± 5%) of receptor sites, and at 10 μmol/L, they all fully saturate the population of receptors. At such concentration, the FRET efficacy for fluorophores randomly distributed in the solution is insignificant and the measurements of FRET for the receptor bound ligand can be performed under equilibrium conditions, with saturating concentrations of the ligand present in the solution.

These concentrations are thus used in following experiments to determine efficiencies of fluorescence energy transfer at comparable receptor sites occupancies, namely saturation.

TmR-ant was able to quench the GFP fluorescence, with a Kd equal to 9.6 nmol/L as determined from FRET amplitude for 3 to 300 nmol/L TmR-ant (Fig. 4; Table 1). At 100 nmol/L the receptor population is close to saturation, which is the concentration used to determine the efficiency in fluorescence energy transfer from GFP to TmR.

Determination of FRET efficacies and estimation of GFP-TxR/TmR separation

Determination of efficacies of FRET between GFP and bound fluorescent NKA derivatives was carried out by measuring variations of donor (GFP) emission amplitude in the presence and absence of a saturating concentration of ligand. Figure 5 illustrates how variation of GFP fluorescence varies in the presence of 0.3 μmol/L TxR1-NKA or 1 μmol/L of TxR4-NKA, TxR7-NKA or TxR10-NKA (Fig. 5). It is clear from both association and dissociation traces that the amplitude of GFP fluorescence variation is progressively smaller when TxR is moved along NKA from position 1–10. All quantitative measurements of fluorescence variation at 510 nm were carried out on dissociation traces recorded after addition of an excess (10 μmol/L) of SR 48968 (Fig. 5). The resulting maximal fluorescence variation (Table 2) was corrected for cell autofluorescence to determine efficiency (E) of energy transfer and separation between GFP and TxR. The shortest mean distance separating GFP from TxR is found when the TxR is positioned at the N-terminal of NKA (46 ± 1 Å). When TxR is linked to position 4, 7 or 10, the corresponding distances are 54 ± 1 Å, 59 ± 1 Å and 68 ± 1 Å, respectively (Table 2).

When 100 nmol/L TmR-ant is present, a concentration at which saturation of receptor sites is reached, 40 ± 1% of the specific-GFP fluorescence is quenched. This corresponds to a distance of 55 ± 1 Å separating the two fluorophores (Table 2).

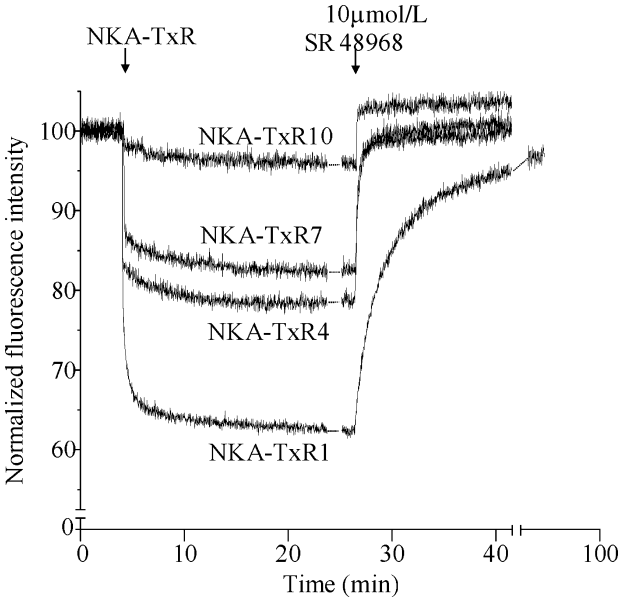

Fig. 5 Fluorescence resonance energy transfer traces used for distance calculation. A suspension of 2×10^6 human embryonic kidney 293 cells stably expressing green fluorescent protein (GFP) -NK2 receptor was irradiated at 470 nm and the fluorescence measured at 510 nm. After 5 min Texas red-neurokinin A (TxR-NKA) analogue was added to finally 300 nmol/L (TxR1-NKA) or 1 μmol/L (TxR4- , TxR7- and TxR10-NKA) concentration, and the fluorescence monitored for up to 25 min until equilibrium reached. To release the receptor bound TxR-NKA, 10 μmol/L SR48968 was added and the dissociation was followed. The traces are normalized to the intensity of cells alone (time 0–5 min).

Discussion

In this study, we investigate the potential structure of the complex formed between NKA and its cognate NK2R. We use FRET to determine distances between GFP grafted to the aminoterminal domain of the receptor and TxR linked to various positions of NKA. The mean distance estimated from efficiency of FRET for each NKA peptide, significantly varies from 46 to 69 Å when TxR is moved stepwise from position 1 to 4, 7 or 10 along the NKA sequence.

These distances are compatible with the dimensions of the receptor-GFP construct. Indeed, according to rhodopsin structure, the size of the receptor itself is approximately 30 Å × 40 Å in the plane of the membrane, and ∼80 A thick. For GFP, the dimensions are in the order of 35 × 25 Å. Further assuming that the N-terminal end of the receptor, may adopt an extended structure, the GFP fluorophore might be up to 100 Å away from the helical bundle of the receptor.

The GFP-TxR distance found for each fluorescent NKA analogue monotonically increases from position 1 (46 Å) to 4 (55 Å), 7 (59 Å) and 10 (68 Å). These data support that, when bound to the receptor, the peptide adopts an extended structure. Indeed, the fluorophore of bound NKA-TxR1 appears to be separated from that of TxR10 by at least 22 Å. For comparison, NKA is roughly 30 Å long in an extended conformation and 10 Å separate the alpha-carbons of residue 1 from 4, 4 from 7 and 7 from 10.

Thus, the measured distances do not support a hairpin conformation of NKA. Also, there is no evidence in favour of a partly helical structure involving residues six to nine as was detected for NKA in the presence of micelles (Whitehead *et al.* 1998).

Although the measured distances are reasonable in terms of molecular dimensions, they are not sufficient to correctly orientate NKA relative to the NK2R. This is essentially due to the lack of constraints on GFP position relative to the receptor. In order to propose a model of the complex, we include the previously described fluorescent peptide TmR-ant in the study. The position of the fluorophore

Table 2 Distance calculation between fluorescent NK2R ligands and GFP-NK2R

	% Maximal fluorescence extinction				Distance (A*)		
	Total fluorescence		GFP-specific				
Ligand		SEM		SEM		SEM	*N*
TxR1-NKA	37.8	0.9	49.6	1.3	46	1	18
TxR4-NKA	21.7	0.8	28.6	0.6	54	1	9
TxR7-NKA	15.8	0.9	20.8	0.8	59	1	9
TxR10-NKA	7.9	0.3	9.9	0.3	68	1	6
TmR-ant	28.9	0.9	40.3	0.9	55	1	6

*Angström

Total: Directly measured FRET intensity as the difference in fluorescence intensity at 510 nm for GFP-NK2R expressing cells in equilibrium with saturating concentrations of TxR-NKA or TmR-ant and the fluorescence intensity after dissociation with 10 μmol/L SR48968 relative to the fluorescence from the GFP-NK2R cells without ligand. GFP-specific (equal to E in distance calculation). Total intensity corrected for non-specific fluorescence corresponding to non-transfected cells. Distance: Distance between GFP and TxR when ligand is receptor bound, calculated from the E-values in second column. The values are average for values found in at least 5 independent experiments.

FRET, fluorescence resonance energy transfer; GFP, green fluorescent protein; TxR, Texas red; TmR-ant, TmR-antagonist; NKA, neurokinin A.

relative to the receptor has been well established, in the bound form of the (Turcatti *et al.* 1996, 1997) and the distance determined to GFP delimits the statistically most significant position of GFP relative to the receptor. In the previous study, TmR-ant peptide was used as an energy acceptor of the nitro benzoxa-diazole (NBD) fluorescent group. The NBD group was incorporated at different positions in six NK2R mutants and pairwise distances separating TmR from NBD were determined. The fluorophore was found to protrude between the TM5 and -6 at the interface between lipid and solvent with the peptide most likely inserted between transmembrane helices 3, 5, 6 and 7. In our work, we determined that the distance from GFP to TmR is 55 Å.

The three dimensional model of the NK2R is based on rhodopsin structure (Palczewski *et al.* 2000) (Fig. 6). After generating the NK2R model, NKA is docked into the protein taking into account appropriate hydrophobic interactions and space (see materials and methods), and the possibility to link the TxR fluorophore on the selected positions 1, 4 7 and 10. Additional pieces of information which are used to constrain the model are NKA analogue binding studies, mutagenesis data from NK2R (Bhogal *et al.* 1994; Renzetti *et al.* 1999; Bremer *et al.* 2000; Giolitti *et al.* 2000), as well as mutagenesis and photoaffinity labelling data obtained on the closely related NK1-receptor (Li *et al.* 1995; Turcatti *et al.* 1997; Holst *et al.* 1998). The resulting NK2R model correctly accounts for all but one inter-aminoacid distances proposed by Turcatti and colleagues (Turcatti *et al.* 1996, 1997), supporting that the NK2R structure fits into the rhodopsin template. Second, the model accounts for the capacity of the receptor, bearing a cysteine residue at position 297 (TM7), to establish covalent bonds with NKA containing a cysteine at position 10 (Labrou *et al.* 2001). In our modelling of the NKA-NK2R complex, we find it possible to place fluorophores outside the helical bundle in such a way that all five measured distances to GFP fit with experimentally determined values.

In the modelled NKA-NK2R complex, NKA is rather linear with the N-terminal part situated close to the receptor surface, in the vicinity of residues belonging to the extracellular loop 2 and N-terminus of the receptor. NKA residue 4 is in the vicinity of extracellular loop 2 and of the top of TM7. Residue 7 is located close to receptor residues Ile114, Met117, Val182, Tyr266 and Phe270. The C-terminal amino acid of NKA is more deeply buried in the receptor structure, close to residues Met117, Tyr266, Trp263, Phe293 and Met297. This position is similar to the site where retinal forms a Schiff base with lysine 296 in rhodopsin, about one-third down in the helical structure of the receptor (Palczewski *et al.* 2000).

The finding that the C-terminus of NKA is not located at the surface of the NK2R may seem contradictory with experimental data obtained with NK1 receptor showing that

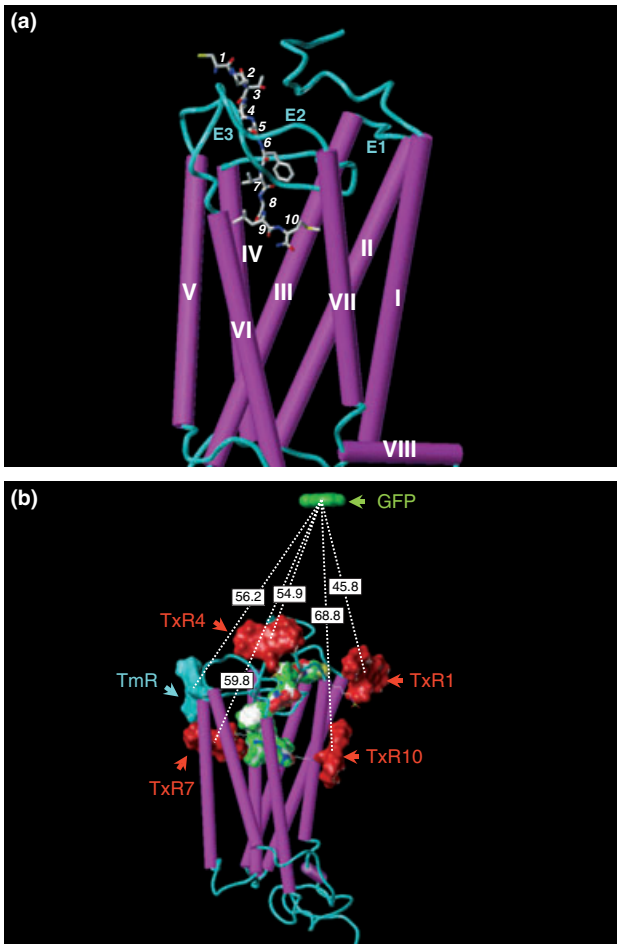

Fig. 6 (a) Three-dimensional model of neurokinin A (NKA) bound to the NK2 receptor (NK2R). The eight alpha-helices of the NK2R are displayed as magenta cylinders and labelled from I–VIII. Intra- and extra-cellular loops (E1–E3) connecting α-helices are represented by cyan tubes. The NKA peptide is displayed as sticks and labelled at every C-α atom from 1 to 10. The following colour code is used for peptide atoms: white, carbon atoms; blue, nitrogen atoms; red, oxygen atoms; yellow, sulphur atoms. (b) Interaction model between the Texas red-labelled NKA and the NK2R-green fluorescent protein (GFP) fusion protein. The GFP chromophore, displayed by a green surface is located within experimentally determined intermolecular distances from 4 positions of NKA (1, 4, 7 and 10) labelled with a Texas red fluorescent moiety (red surface). NKA is displayed by a colour-coded surface (white, carbon atoms; blue, nitrogen atoms; red, oxygen atoms; yellow, sulphur atoms; cyan, hydrogen atoms). For comparison purpose, the position of a TmR group (cyan surface), as previously proposed in a previous model (Turcatti *et al.* 1996) is displayed. Key intermolecular distances, in Å, are displayed in white boxes.

the C-terminus of SP is exposed to the extracellular medium (Turcatti *et al.* 1997). Although the introduction of a fluorophore at the C-terminus of NKA may result in a reorientation of the C-terminal end of NKA, it is well documented that C-terminal parts of NKA and SP do not

contribute identically to signalling on their respective receptors (Regoli *et al.* 1994).

Altogether, the proposed position of NKA is in good agreement with site-directed mutagenesis data showing that agonists and the competitive antagonist SR 48968 binding pocket is surrounded by residues from the 253–295 domain mainly with amino acid 289 (Gether *et al.* 1993a,b; Huang *et al.* 1995; Labrou *et al.* 2001) within the receptor monomer. The present experimental determination of bound ligand structure thus proves useful to decipher areas of the receptor protein that contribute to the binding pocket of natural ligands. It should bring valuable information to understand ligand selectivity and possibly to set up efficient structure-assisted drug design approaches.

Acknowledgements

We thank F. Pattus for helpful comments. This work was supported by the Centre National de la Recherche Scientifique, the Association pour la Recherche sur le Cancer, the Fondation pour le Recherche Médicale, the Ligue Nationale Contre le Cancer (Comité du Haut-Rhin), The Agence Nationale pour la Recherche sur le SIDA and Glaxo Welcome (fellowship to SZ).

References

Beaujouan J. C., Saffroy M., Torrens Y. and Glowinski J. (2000) Different subtypes of tachykinin NK(1) receptor binding sites are present in the rat brain. *J. Neurochem.* **75**, 1015–1026.

Bhogal N., Donnelly D. and Findlay J. B. (1994) The ligand binding site of the neurokinin 2 receptor Site-directed mutagenesis and identification of neurokinin A binding residues in the human neurokinin 2 receptor. *J. Biol. Chem.* **269**, 27 269–27 274.

Bradshaw C. G., Ceszkowski K., Turcatti G., Beresford I. J. and Chollet A. (1994) Synthesis and characterization of selective fluorescent ligands for the neurokinin NK2 receptor. *J. Med. Chem.* **37**, 1991–1995.

Bremer A. A., Leeman S. E. and Boyd N. D. (2000) The common C-terminal sequences of substance P and neurokinin A contact the same region of the NK-1 receptor. *FEBS Lett.* **486**, 43–48.

Cheng Y.-C. and Prussoff W. H. (1973) Relationship between the inhibition constant (Ki) and the concentration of inhibitor which causes 50 per cent inhibition (IC50) of an enzymatic reaction. *Biochem. Pharmacol.* **22**, 3099–3108.

Debeljuk L., Ghosh P. and Bartke A. (1990) Neurokinin A levels in the hypothalamus of rats and mice, effects of castration, gonadal steroids and expression of heterologous growth hormone genes. *Brain Res. Bull.* **25**, 717–721.

Fraternali F., Do Q. T., Doan B. T., Atkinson R. A., Palmas P., Sklenar V., Safar P., Wildgoose P., Strop P. and Saudek V. (1998) Mapping the active site of factor Xa by selective inhibitors: an NMR and MD study. *Proteins* **30**, 264–274.

Gao X. and Wong T. C. (1999) The study of the conformation and interaction of two tachykinin peptides in membrane mimicking systems by NMR spectroscopy and pulsed field gradient diffusion. *Biopolymers* **50**, 555–568.

Gembitsky D. S., Murnin M., Otvos F. L., Allen J., Murphy R. F. and Lovas S. (1999) Importance of the aromatic residue at position 6 of [Nle(10)]neurokinin A(4-10) for binding to the NK-2 receptor and receptor activation. *J. Med. Chem.* **42**, 3004–3007.

Gether U., Yokota Y., Emonds-Alt X., Breliere J. C., Lowe J. A. d., Snider R. M., Nakanishi S. and Schwartz T. W. (1993a) Two nonpeptide tachykinin antagonists act through epitopes on corresponding segments of the NK1 and NK2 receptors. *Proc. Natl Acad. Sci. USA* **90**, 6194–6198.

Gether U., Johansen T. E., Snider R. M., Lowe J. A. d., Nakanishi S. and Schwartz T. W. (1993b) Different binding epitopes on the NK1 receptor for substance P and non- peptide antagonist. *Nature* **362**, 345–348.

Giolitti A., Cucchi P., Renzetti A. R., Rotondaro L., Zappitelli S. and Maggi C. A. (2000) Molecular determinants of peptide and non-peptide NK-2 receptor antagonists binding sites of the human tachykinin NK-2 receptor by site- directed mutagenesis. *Neuropharmacology* **39**, 1422–1429.

Griebel G. (1999) Is there a future for neuropeptide receptor ligands in the treatment of anxiety disorders? *Pharmacol. Ther.* **82**, 1–61.

Heiden W., Moeckel G. and Brickmann J. (1993) A new approach to analysis and display of local lipophilicity/hydrophilicity mapped on molecular surfaces. *J. Comput. Aided Mol. Des.* **7**, 503–514.

Heim R. and Tsien R. Y. (1996) Engineering green fluorescent protein for improved brightness, longer wavelengths and fluorescence resonance energy transfer. *Curr. Biol.* **6**, 178–182.

Holst B., Zoffmann S., Elling C. E., Hjorth S. A. and Schwartz T. W. (1998) Steric hindrance mutagenesis versus alanine scan in mapping of ligand binding sites in the tachykinin NK1 receptor. *Mol. Pharmacol.* **53**, 166–175.

Huang R. R., Vicario P. P., Strader C. D. and Fong T. M. (1995) Identification of residues involved in ligand binding to the neurokinin-2 receptor. *Biochemistry* **34**, 10 048–10 055.

Ilien B., Franchet C., Bernard P., Morisset S., Weill C. O., Bourguignon J. J., Hibert M. and Galzi J. L. (2003) Fluorescence resonance energy transfer to probe human M1 muscarinic receptor structure and drug binding properties. *J. Neurochem.* **85**, 768–778.

Kallal L. and Benovic J. L. (2000) Using green fluorescent proteins to study G-protein-coupled receptor localization and trafficking. *Trends Pharmacol. Sci.* **21**, 175–180.

Labrou N. E., Mello L. V., Rigden D. J., Keen J. N. and Findlay J. B. (1999) Structure-activity studies on cysteine-substituted neurokinin A analogs. *Peptides* **20**, 795–801.

Labrou N. E., Bhogal N., Hurrell C. R. and Findlay J. B. (2001) Interaction of Met297 in the seventh transmembrane segment of the tachykinin NK2 receptor with neurokinin A. *J. Biol. Chem.* **276**, 37 944–37 949.

Lakey J. H., Baty D. and Pattus F. (1991) Fluorescence energy transfer distance measurements using site-directed single cysteine mutants. The membrane insertion of colicin A.. *J. Mol. Biol.* **218**, 639–653.

Lecat S., Bucher B., Mely Y. and Galzi J. L. (2002) Mutations in the extracellular amino-terminal domain of the NK2 neurokinin receptor abolish cAMP signaling but preserve intracellular calcium responses. *J. Biol. Chem.* **277**, 42 034–42 048.

Li Y. M., Marnerakis M., Stimson E. R. and Maggio J. E. (1995) Mapping peptide-binding domains of the substance P (NK-1) receptor from P388D1 cells with photolabile agonists. *J. Biol. Chem.* **270**, 1213–1220.

Lordal M., Navalesi G., Theodorsson E., Maggi C. A. and Hellstrom P. M. (2001) A novel tachykinin NK2 receptor antagonist prevents motility-stimulating effects of neurokinin A in small intestine. *Br. J. Pharmacol.* **134**, 215–223.

Neugebauer V., Rumenapp P. and Schaible H. G. (1996) The role of spinal neurokinin-2 receptors in the processing of nociceptive information from the joint and in the generation and maintenance of inflammation-evoked hyperexcitability of dorsal horn neurons in the rat. *Eur. J. Neurosci.* **8**, 249–260.

Palczewski K., Kumasaka T., Hori T. *et al.* (2000) Crystal structure of rhodopsin: A G protein-coupled receptor [see comments]. *Science* **289**, 739–745.

Regoli D., Rhaleb N. E., Dion S., Tousignant C., Rouissi N., Jukic D. and Drapeau G. (1990) Neurokinin A A pharmacological study. *Pharmacol. Res.* **22**, 1–14.

Regoli D., Boudon A. and Fauchere J. L. (1994) Receptors and antagonists for substance P and related peptides. *Pharmacol. Rev.* **46**, 551–599.

Renzetti A. R., Catalioto R. M., Criscuoli M., Cucchi P., Ferrer C., Giolitti A., Guelfi M., Rotondaro L., Warner F. J. and Maggi C. A. (1999) Relevance of aromatic residues in transmembrane segments V to VII for binding of peptide and nonpeptide antagonists to the human tachykinin NK(2) receptor. *J. Pharmacol. Exp. Ther.* **290**, 487–495.

Saffroy M., Torrens Y., Glowinski J. and Beaujouan J. C. (2003) Autoradiographic distribution of tachykinin NK2 binding sites in the rat brain: comparison with NK1 and NK3 binding sites. *Neuroscience* **116**, 761–773.

Sasai Y. and Nakanishi S. (1989) Molecular characterization of rat substance K receptor and its mRNAs. *Biochem. Biophys. Res. Commun.* **165**, 695–702.

Sternini C., Anderson K., Frantz G., Krause J. E. and Brecha N. (1989) Expression of substance P/neurokinin A-encoding preprotachykinin messenger ribonucleic acids in the rat enteric nervous system. *Gastroenterology* **97**, 348–356.

Turcatti G., Vogel H. and Chollet A. (1995) Probing the binding domain of the NK2 receptor with fluorescent ligands: evidence that heptapeptide agonists and antagonists bind differently. *Biochemistry* **34**, 3972–3980.

Turcatti G., Nemeth K., Edgerton M. D., Meseth U., Talabot F., Peitsch M., Knowles J., Vogel H. and Chollet A. (1996) Probing the structure and function of the tachykinin neurokinin-2 receptor through biosynthetic incorporation of fluorescent amino acids at specific sites. *J. Biol. Chem.* **271**, 19 991–19 998.

Turcatti G., Zoffmann S., Lowe J. A.III., Drozda S. E., Chassaing G., Schwartz T. W. and Chollet A. (1997) Characterization of non-peptide antagonist and peptide agonist binding sites of the NK1 receptor with fluorescent ligands. *J. Biol. Chem.* **272**, 21 167–21 175.

Van Rhee A. M., Fischer B., Van Galen P. J. and Jacobson K. A. (1995) Modelling the P2Y purinoceptor using rhodopsin as template. *Drug Des. Discov.* **13**, 133–154.

Van Schoor J., Joos G. F., Chasson B. L., Brouard R. J. and Pauwels R. A. (1998) The effect of the NK2 tachykinin receptor antagonist SR 48968 (saredutant) on neurokinin A-induced bronchoconstriction in asthmatics. *Eur. Respir. J.* **12**, 17–23.

Vollmer J. Y., Alix P., Chollet A., Takeda K. and Galzi J. L. (1999) Subcellular compartmentalization of activation and desensitization of responses mediated by NK2 neurokinin receptors. *J. Biol. Chem.* **274**, 37 915–37 922.

Whitehead T. L., McNair S. D., Hadden C. E., Young J. K. and Hicks R. P. (1998) Membrane-induced secondary structures of neuropeptides: a comparison of the solution conformations adopted by agonists and antagonists of the mammalian tachykinin NK1 receptor. *J. Med. Chem.* **41**, 1497–1506.

Zhang Y., Lu L., Furlonger C., Wu G. E. and Paige C. J. (2000) Hemokinin is a hematopoietic-specific tachykinin that regulates B lymphopoiesis. *Nat. Immunol.* **1**, 392–397.

Zimmer A., Zimmer A. M., Baffi J., Usdin T., Reynolds K., Konig M., Palkovits M. and Mezey E. (1998) Hypoalgesia in mice with a targeted deletion of the tachykinin 1 gene. *Proc. Natl Acad. Sci. USA* **95**, 2630–2635.

